

1 **Erosion of somatic tissue identity with loss of the X-linked**
2 **intellectual disability factor KDM5C**

3

4 Katherine M. Bonefas, Ilakkiya Venkatachalam, and Shigeki Iwase.

5 **Abstract**

6 Mutations in numerous chromatin-modifying enzymes cause neurodevelopmental disorders (NDDs).
7 Loss of repressive chromatin regulators can lead to the aberrant transcription of tissue-specific genes
8 outside of their intended context, however the mechanisms and consequences of their dysregulation are
9 largely unknown. Here, we explored this cellular identity crisis in NDDs by investigating lysine demethylase
10 5c (KDM5C), an eraser of histone 3 lysine 4 di and tri-methylation (H3K4me2/3), in tissue identity. We
11 found male *Kdm5c* knockout (-KO) mice, which recapitulate key behavioral phenotypes of Claes-Jensen
12 X-linked intellectual disability, aberrantly expresses many liver, muscle, ovary, and testis genes within the
13 amygdala and hippocampus. Gonad-enriched genes expressed in the *Kdm5c*-KO brain were typically
14 unique to germ cells, indicating an erosion of the soma-germline boundary. Germline genes are usually
15 decommissioned in somatic lineages in the post-implantation epiblast, yet *Kdm5c*-KO epiblast-like cells
16 (EpiLCs) aberrantly expressed key regulators of germline identity and meiosis, including *Dazl* and *Stra8*.
17 Germline gene suppression is sexually dimorphic, as female EpiLCs required a higher dose of KDM5C to
18 maintain germline gene suppression. Using a curated list of mouse germline-enriched genes, we found
19 KDM5C is selectively recruited to a subset of germline gene promoters that contain CpG islands (CGIs)
20 to facilitate DNA CpG methylation (CpGme) during ESC to EpiLC differentiation. However, late stage
21 spermatogenesis genes devoid of promoter CGIs can also become activated in *Kdm5c*-KO cells via ectopic
22 activation by RFX transcription factors. Thus, distinct suppressive mechanisms are recruited to different
23 germline gene classes and ectopic germline transcriptional programs can mirror germ cell development
24 within somatic tissues.

25 **Introduction**

26 A single genome holds the instructions to generate the myriad of cell types found within an organism.
27 This is, in part, accomplished by chromatin regulators that can either promote or impede lineage-specific

28 gene expression through DNA and histone modifications^{1–5}. Human genetic studies revealed mutations in
29 chromatin regulators are a major cause of neurodevelopmental disorders (NDDs)⁶ and many studies have
30 identified their importance for regulating brain-specific transcriptional programs. Loss of some chromatin
31 regulators can also result in the ectopic expression of tissue-specific genes outside of their target environment,
32 such as the misexpression of liver-specific genes within adult neurons⁷. However, the mechanisms underlying
33 ectopic gene expression and its impact upon neurodevelopment are poorly understood.

34 To elucidate the role of tissue identity in chromatin-linked NDDs, it is essential to first characterize the
35 nature of the dysregulated genes and the molecular mechanisms governing their de-repression. Here we
36 focus on lysine demethylase 5C (KDM5C, also known as SMCX or JARID1C), which erases histone 3 lysine
37 4 di- and trimethylation (H3K4me2/3), a permissive chromatin modification enriched at gene promoters⁸.
38 Pathogenic mutations in *KDM5C* cause Intellectual Developmental Disorder, X-linked, Syndromic, Claes-
39 Jensen Type (MRXSCJ, OMIM: 300534). MRXSCJ is more common and severe in males and its neurological
40 phenotypes include intellectual disability, seizures, aberrant aggression, and autistic behaviors^{9–11}. Male
41 *Kdm5c* knockout (-KO) mice recapitulate key MRXSCJ phenotypes, including hyperaggression, increased
42 seizure propensity, and learning impairments^{12,13}. RNA sequencing (RNA-seq) of the *Kdm5c*-KO hippocam-
43 pus surprisingly revealed ectopic expression of some germline genes within the brain¹³. However, it is unclear
44 if other tissue-specific genes are aberrantly transcribed with KDM5C loss, at what point in development
45 germline gene misexpression begins, and what mechanisms underlie their dysregulation.

46 Distinguishing between germ cells and somatic cells is a key feature of multicellularity¹⁴ that occurs
47 during early embryogenesis in many metazoans¹⁵. In mammals, chromatin regulators are crucial for
48 decommissioning germline genes during the transition from naïve to primed pluripotency. Initially, germline
49 gene promoters gain repressive histone H2A lysine 119 monoubiquitination (H2AK119ub1)¹⁶ and histone 3
50 lysine 9 trimethylation (H3K9me3)^{16,17} in embryonic stem cells (ESCs) and are then decorated with DNA
51 CpG methylation (CpGme) in the post-implantation embryo^{17–19}. The contribution of KDM5C to this process
52 remains unclear. Furthermore, studies on germline gene repression have primarily been conducted in males
53 and focused on marker genes important for germ cell development rather than germline genes as a whole,
54 given the lack of a curated list for germline-enriched genes. Therefore, it is unknown if the mechanism
55 of repression differs between sexes or for certain classes of germline genes, e.g. meiotic genes versus
56 spermatid differentiation genes.

57 To illuminate KDM5C's role in tissue identity, here we characterized the aberrant expression of tissue-
58 enriched genes within the *Kdm5c*-KO brain and epiblast-like stem cells (EpiLCs), an *in vitro* model of the
59 post-implantation embryo. We curated list of mouse germline-enriched genes, which enabled genome-wide
60 analysis of germline gene silencing mechanisms for the first time. Based on the data presented below, we
61 propose KDM5C plays a fundamental, sexually dimorphic role in the development of tissue identity during
62 early embryogenesis, including the establishment of the soma-germline boundary.

63 **Results**

64 **Tissue-enriched genes are aberrantly expressed in the *Kdm5c*-KO brain**

65 Previous RNA sequencing (RNA-seq) of the adult male *Kdm5c*-KO hippocampus revealed ectopic
66 expression of some germline genes unique to the testis¹³. It is currently unknown if the testis is the only
67 tissue type misexpressed in the *Kdm5c*-KO brain. We thus characterized the role of KDM5C in brain tissue
68 identity by systematically assessing the dysregulation of genes enriched in 17 mouse tissues²⁰. We analyzed
69 tissue-specific differentially expressed genes (DEGs) in our published mRNA-seq datasets²¹ of the adult
70 amygdala and hippocampus from wild-type and constitutive *Kdm5c*-KO male mice (DESeq2²², log2 fold
71 change > 0.5, q < 0.1).

72 We found a large proportion of significantly upregulated genes within the *Kdm5c*-KO brain are typically
73 enriched within non-brain tissues (Amygdala: 35%, Hippocampus: 24%) (Figure 1A-B). For both the
74 amygdala and hippocampus, the majority of tissue-enriched (DEGs) were testis genes (Figure 1A-C). Even
75 though the testis has the largest total number of tissue-biased genes (2,496 genes) compared to any other
76 tissue, testis-biased DEGs were significantly enriched for both brain regions (Amygdala p = 1.83e-05, Odds
77 Ratio = 5.13; Hippocampus p = 4.26e-11, Odds Ratio = 4.45, Fisher's Exact Test). One example of a
78 testis-enriched gene misexpressed in the *Kdm5c*-KO brain is *FK506 binding protein 6* (*Fkbp6*), a known
79 regulator of PIWI-interacting RNAs (piRNAs) and meiosis^{23,24} (Figure 1C).

80 Interestingly, we also observed significant enrichment of ovary-biased DEGs in both the amygdala and
81 hippocampus (Amygdala p = 0.00574, Odds Ratio = 18.7; Hippocampus p = 0.048, Odds Ratio = 5.88,
82 Fisher's Exact) (Figure 1A-B). Ovary-enriched DEGs included *Zygotic arrest 1* (*Zar1*), which sequesters
83 mRNAs in oocytes for meiotic maturation²⁵ (Figure 1D). Given that the *Kdm5c*-KO mice we analyzed are
84 male, these data demonstrate that the ectopic expression of gonad-enriched genes is independent of
85 organismal sex.

86 Although not consistent across brain regions, we also found significant enrichment of DEGs biased
87 towards two non-gonadal tissues - the liver (Amygdala p = 0.04, Odds Ratio = 6.58, Fisher's Exact Test) and
88 the muscle (Hippocampus p = 0.01, Odds Ratio = 6.95, Fisher's Exact Test) (Figure 1A-B). *Apolipoprotein*
89 *C-1* (*Apoc1*) a lipoprotein metabolism and transport gene, is among the liver-biased DEG derepressed in both
90 the hippocampus and amygdala²⁶ and its brain overexpression has been implicated in Alzheimer's disease²⁷
91 (Figure 1E).

92 For all *Kdm5c*-KO tissue-enriched DEGs, aberrantly expressed mRNAs are polyadenylated and spliced
93 into mature transcripts (Figure 1C-E). Of note, we observed little to no dysregulation of brain-enriched genes
94 (Amygdala p = 1, Odds Ratio = 1.22; Hippocampus p = 0.74, Odds Ratio = 1.22, Fisher's Exact), despite the
95 fact these are brain samples and the brain has the second highest total number of tissue-enriched genes
96 (708 genes). Altogether, these results suggest the aberrant expression of tissue-enriched genes within the
97 brain is a major effect of KDM5C loss.

98 **Germline genes are misexpressed in the *Kdm5c*-KO brain**

99 *Kdm5c*-KO brain expresses testicular germline genes¹³, however the testis also contains somatic cells that
100 support hormone production and germline functions. To determine if *Kdm5c*-KO results in ectopic expression
101 of somatic testicular genes, we first evaluated the known functions of testicular DEGs through gene ontology.
102 We found *Kdm5c*-KO testis-enriched DEGs had high enrichment of germline-relevant ontologies, including
103 spermatid development (GO: 0007286, p.adjust = 6.2e-12) and sperm axoneme assembly (GO: 0007288,
104 p.adjust = 2.45e-14) (Figure 2A).

105 We then evaluated testicular DEG expression in wild-type testes versus testes with germ cell depletion²⁸,
106 which was accomplished by heterozygous *W* and *Wv* mutations in the enzymatic domain of *c-Kit* (*Kit*^{W/Wv})²⁹.
107 Almost all *Kdm5c*-KO testis-enriched DEGs lost expression with germ cell depletion (Figure 2B). We then
108 assessed testis-enriched DEG expression in a published single cell RNA-seq dataset that identified cell
109 type-specific markers within the testis³⁰. Some *Kdm5c*-KO testis-enriched DEGs were classified as specific
110 markers for different germ cell developmental stages (e.g. spermatogonia, spermatocytes, round spermatids,
111 and elongating spermatids), yet none marked somatic cells (Figure 2C). Together, these data demonstrate
112 that the *Kdm5c*-KO brain aberrantly expresses germline genes, but not somatic testicular genes, reflecting
113 an erosion of the soma-germline boundary.

114 As of yet, research on germline gene silencing mechanisms has focused on a handful of key genes
115 rather than assessing germline gene suppression genome-wide due to the lack of a comprehensive gene list.
116 We therefore generated a list of mouse germline-enriched genes using RNA-seq datasets of *Kit*^{W/Wv} mice
117 that included males and females at embryonic day 12, 14, and 16³¹ and adult male testes²⁸. We defined
118 genes as germline-enriched if their expression met the following criteria: 1) their expression is greater than
119 1 FPKM in wild-type gonads 2) their expression in any non-gonadal tissue of adult wild type mice²⁰ does
120 not exceed 20% of their maximum expression in the wild-type germline, and 3) their expression in the germ
121 cell-depleted gonads, for any sex or time point, does not exceed 20% of their maximum expression in the
122 wild-type germline. These criteria yielded 1,288 germline-enriched genes (Figure 2D), which was hereafter
123 used as a resource to globally characterize germline gene misexpression with *Kdm5c* loss (Supplementary
124 table 1).

125 ***Kdm5c*-KO epiblast-like cells aberrantly express key regulators of germline identity**

126 Germ cells are typically distinguished from somatic cells soon after the embryo implants into the uterine
127 wall^{32,33}, when they are silenced in epiblast stem cells that will differentiate into the ectoderm, mesoderm,
128 and endoderm to form the somatic tissues³⁴. This developmental time point can be modeled *in vitro* through
129 differentiation of naïve embryonic stem cells (nESCs) into epiblast-like stem cells (EpiLCs) (Figure 3A)^{35,36}.
130 While some germline-enriched genes are also expressed in nESCs and in the 2-cell stage³⁷⁻³⁹, they are
131 silenced as they differentiate into EpiLCs^{17,40}. Therefore, we tested if KDM5C was necessary for the initial

132 silencing germline genes in somatic lineages by evaluating the impact of *Kdm5c* loss in male EpiLCs.
133 *Kdm5c*-KO cell morpholgy during ESC to EpiLC differentiation appeared normal (Figure 3B) and EpiLCs
134 properly expressed markers of primed pluripotency, such as *Dnmt3b*, *Fgf5*, *Pou3f1*, and *Otx2* (Figure 3C).
135 We then identified tissue-enriched DEGs in our previously published RNA-seq dataset of wild-type and
136 *Kdm5c*-KO EpiLCs⁴¹ (DESeq2, log2 fold change > 0.5, q < 0.1). Similar to the *Kdm5c*-KO brain, we observed
137 general dysregulation of tissue-enriched genes, with the largest number of genes belonging to the brain and
138 testis, although they were not significantly enriched (Figure 3D). Using our list of mouse germline-enriched
139 genes assembled above, we found 54 germline genes were misexpressed in male *Kdm5c*-KO EpiLCs.

140 We then compared EpiLC germline DEGs to those expressed in the *Kdm5c*-KO brain to determine if
141 germline genes are constitutively dysregulated or change over the course of development. The majority
142 of germline DEGs were unique to either EpiLCs or the brain, with only *Cyct* shared across all tissue/cell
143 types (Figure 3E-F). EpiLCs had particularly high enrichment of meiosis-related gene ontologies (Figure
144 3G), such as meiotic cell cycle process (GO:1903046, p.adjust = 1.59e-08) and meiotic nuclear division
145 (GO:0140013, p.adjust = 9.76e-09). While there was modest enrichment of meiotic gene ontologies in both
146 brain regions, the *Kdm5c*-KO hippocampus primarily expressed late-stage spermatogenesis genes involved
147 in sperm axoneme assembly (GO:0007288, p.adjust = 0.00621) and sperm motility (GO:0097722, p.adjust =
148 0.00612).

149 Notably, DEGs unique to *Kdm5c*-KO EpiLCs included key drivers of germline identity, such as *Stimulated*
150 *by retinoic acid 8* (*Stra8*: log2 fold change = 3.7, q = 2.05e-26) and *Deleted in azoospermia like* (*Dazl*: log2
151 fold change = 3.16, q = 4.08e-06) (Figure 3H). These genes are typically expressed when primordial germ
152 cells (PGCs) are committed to the germline fate, but are also expressed later in life to trigger meiotic gene
153 expression programs⁴²⁻⁴⁴. Of note, some germline genes, including *Dazl*, are also expressed in the two-cell
154 embryo^{38,45}. However, we did not see derepression of two-cell stage-specific genes, like *Duxf3* (*Dux*) (log2
155 fold change = -0.282, q = 0.337) and *Zscan4d* (log2 fold change = 0.25, q = 0.381) (Figure 3H), indicating
156 *Kdm5c*-KO EpiLCs do not revert back to a 2-cell-like state. Altogether, *Kdm5c*-KO EpiLCs expressing key
157 drivers of germline identity and meiosis while the brain primarily expresses spermiogenesis genes indicate
158 germline gene misexpression parallels germline development during proper *Kdm5c*-KO differentiation.

159 **Female epiblast-like cells have increased sensitivity to germline gene misexpression
160 with *Kdm5c* loss**

161 It is currently unknown if the misexpression of germline genes is influenced by sex, as previous studies
162 on germline gene repressors have focused on males^{16-18,46,47}. Sex is particularly pertinent in the case
163 of KDM5C because it partially escapes X chromosome inactivation (XCI), resulting in a higher dosage in
164 females⁴⁸⁻⁵¹. We therefore explored the impact of chromosomal sex upon germline gene suppression by
165 comparing their dysregulation in male *Kdm5c* hemizygous knockout (XY *Kdm5c*-KO), female homozygous

166 knockout (XX *Kdm5c*-KO), and female heterozygous knockout (XX *Kdm5c*-HET) EpiLCs.⁴¹.
167 Homozygous and heterozygous *Kdm5c* knockout females expressed over double the number of germline-
168 enriched genes than hemizygous males (Figure 4A). While the majority of germline DEGs in *Kdm5c*-KO
169 males were also dysregulated in females (74%), many were male-specific and female-specific, such as
170 *Tktl2* and *Esx1* (Figure 4B). We then compared the known functions of germline genes dysregulated only in
171 females (XX only - dysregulated in XX *Kdm5c*-KO, XX *Kdm5c*-HET, or both), only in males (XY only), or in
172 all samples (shared) (Figure 4C). Female-specific germline DEGs were enriched for meiotic (GO:0051321
173 meiotic cell cycle) and flagellar (GO:0003341 cilium movement) functions, while male-specific DEGs had
174 roles in mitochondrial and cell signaling (GO:0070585 protein localization to mitochondrion). Germline
175 transcripts expressed in both sexes were enriched for meiotic (GO:0140013 meiotic nuclear division) and
176 egg-specific functions (GO:0007292 female gamete generation).

177 The majority of germline genes expressed in both sexes had a greater log2 fold change in females
178 compared to males (Figure 4D-F). This increased degree of dysregulation in females, along with the
179 increased total number of germline genes, indicates females are more sensitive to losing KDM5C-mediated
180 germline gene suppression. Female sensitivity could be due to impaired XCI in *Kdm5c* mutants⁴¹, as many
181 spermatogenesis genes lie on the X chromosome^{52,53}. However, female germline DEGs were not biased
182 towards the X chromosome and had a similar overall proportion of X chromosome DEGs compared to
183 males (XY *Kdm5c*-KO - 10.29%, XX *Kdm5c*-HET - 7.43%, XX *Kdm5c*-KO - 10.59%) (Figure 4G). The
184 majority of germline DEGs instead lie on autosomes for both male and female *Kdm5c* mutants (Figure 4G).
185 Thus, while female EpiLCs are more prone to germline gene misexpression with KDM5C loss, it is likely
186 independent of XCI defects.

187 **Germline gene misexpression in *Kdm5c* mutants is independent of germ cell sex**

188 Although many germline genes have shared functions in the male and female germline, some have
189 unique or sex-biased expression. Therefore, we wondered if *Kdm5c* mutant males would primarily express
190 sperm genes while mutant females primarily expressed egg genes. To comprehensively assess whether
191 germline gene sex corresponds with *Kdm5c* mutant sex, we first filtered our list of germline-enriched genes
192 for egg and sperm-biased genes (Figure 4H). We defined germ cell sex-biased genes as those whose
193 expression in the opposite sex, at any time point, is no greater than 20% of the gene's maximum expression
194 in a given sex. This yielded 67 egg-biased, 1,024 sperm-biased, and 197 unbiased germline-enriched genes.
195 We found egg, sperm, and unbiased germline genes were dysregulated in all *Kdm5c* mutants at similar
196 proportions (Figure 4I-J). Furthermore, germline genes dysregulated exclusively in either male or female
197 mutants were also not biased towards their corresponding germ cell sex (Figure 4I). Altogether, these results
198 demonstrate sex differences in germline gene dysregulation is not due to sex-specific activation of sperm or
199 egg transcriptional programs.

200 **KDM5C binds to a subset of germline gene promoters during early embryogenesis**

201 KDM5C binds to the promoters of several germline genes in embryonic stem cells (ESCs) but its binding
202 is absent in neurons¹³. However, the lack of a comprehensive list of germline-enriched genes prohibited
203 genome-wide characterization of KDM5C binding at germline gene promoters. Thus, it is unclear if KDM5C
204 is enriched at germline gene promoters, what types of germline genes KDM5C regulates, and if its binding is
205 maintained at any germline genes in neurons.

206 To address these questions, we analyzed KDM5C chromatin immunoprecipitation followed by DNA
207 sequencing (ChIP-seq) datasets in EpiLCs⁴¹ and primary forebrain neuron cultures (PNCs)¹². EpiLCs had a
208 higher total number of high-confidence KDM5C peaks than PNCs (EpiLCs: 5,808, PNCs: 1,276, MACS2 q <
209 0.1 and fold enrichment > 1). KDM5C was primarily localized to gene promoters in both cell types (EpiLCs:
210 4,190, PNCs: 745 ± 500bp from the TSS), although PNCs showed increased localization to non-promoter
211 regions (Figure 5A).

212 The majority of promoters bound by KDM5C in PNCs were also bound in EpiLCs (513 shared promoters),
213 however a large portion of gene promoters were only bound by KDM5C in EpiLCs (3,677 EpiLC only
214 promoters) (Figure 5B). Genes bound by KDM5C in both PNCs and EpiLCs were enriched for functions
215 involving nucleic acid turnover, such as deoxyribonucleotide metabolic process (GO:0009262, p.adjust =
216 8.28e-05) (Figure 5C). Germline-specific ontologies were only enriched in KDM5C-bound promoters unique
217 to EpiLCs, such as meiotic nuclear division (GO: 0007127 p.adjust = 6.77e-16) and meiotic cell cycle process
218 (GO:1903046, p.adjust = 5.05e-16) (Figure 5C). There were no ontologies significantly enriched for genes
219 bound by KDM5C only in PNCs. Using our mouse germline gene list, we observed evident KDM5C signal
220 around the TSS of many germline genes in EpiLCs, but not in PNCs (Figure 5D). Based on our ChIP-seq
221 peak cut-off criteria, KDM5C was highly enriched at 211 germline gene promoters in EpiLCs (0.164% of all
222 germline genes) (Figure 5E). Of note, KDM5C was only bound to about one third of *Kdm5c*-KO RNA-seq
223 DEG promoters (EpiLC only DEGs: 36%, Brain only DEGs: 33.3%) (Supplementary figure 1A-C). However,
224 KDM5C was bound to the promoter at 3 out of the 4 genes dysregulated in both the brain and EpiLCs.
225 Representative examples of KDM5C-bound and unbound germline DEGs are *Dazl* and *Stra8*, respectively
226 (Figure 5F). Together, these results demonstrate KDM5C is recruited to a subset of germline genes in EpiLCs,
227 including meiotic genes, but does not directly regulate germline genes in neurons. Furthermore, the majority
228 of germline mRNAs expressed in *Kdm5c*-KO cells are dysregulated independent of direct KDM5C binding to
229 their promoters.

230 Many germline-specific genes are suppressed by the transcription factor heterodimers E2F6/DP1 and
231 MGA/MAX, which respectively bind E2F and E-box motifs^{18,46,47,54,55}. To elucidate if KDM5C is recruited to
232 germline genes by a similar mechanism, we used HOMER⁵⁶ to identify transcription factor motifs enriched at
233 KDM5C-bound or unbound germline gene promoters (TSS ± 500 bp, q-value < 0.1). MAX and E2F6 binding
234 sites were significantly enriched at germline genes bound by KDM5C in EpiLCs, but not at germline genes
235 unbound by KDM5C (MAX q-value: 0.0068, E2F6 q-value: 0.0673, E2F q-value: 0.0917) (Figure 5G). One

236 third of KDM5C-bound promoters contained the consensus sequence for either E2F6 (E2F, 5'-TCCCGC-3'),
237 MGA (E-box, 5'-CACGTG-3'), or both, but only 17% of KDM5C-unbound genes contained these motifs (Figure
238 5H). KDM5C-unbound germline genes were instead enriched for multiple RFX transcription factor binding
239 sites (RFX q-value < 0.0001, RFX2 q-value < 0.0001, RFX5 q-value < 0.0001) (Figure 5I, Supplementary
240 figure 1D). RFX transcription factors bind X-box motifs⁵⁷ to promote ciliogenesis^{58,59} and among them is
241 RFX2, a central regulator of post-meiotic spermatogenesis^{60,61}. Interestingly, RFX2 mRNA is derepressed
242 in *Kdm5c*-KO EpiLCs (Figure 5J), however it is also not a direct target of KDM5C (Supplementary figure
243 1E). Thus, RFX2 is a candidate transcription factor for driving the ectopic expression of KDM5C-unbound
244 germline genes in *Kdm5c*-KO cells.

245 **KDM5C is recruited to CpG islands within germline gene promoters to facilitate *de*
246 *novo* DNA methylation**

247 In the early embryo, germline gene promoters are initially decorated with repressive histone modifications
248 and are then silenced long-term via DNA CpG methylation (CpGme)^{16,17,40,62}. Our results above indicate
249 KDM5C also acts at germline gene promoters during this time period. However, how KDM5C interacts with
250 other germline gene silencing mechanisms is currently unclear. KDM5C is generally thought to suppress
251 transcription through erasure of histone 3 lysine 4 di- and trimethylation (H3K4me2/3)⁸, yet KDM5C's
252 catalytic activity was recently shown to be dispensable for suppressing *Dazl* in undifferentiated ESCs⁴⁵. Since
253 H3K4me3 impedes *de novo* CpGme placement^{63,64}, KDM5C's catalytic activity may instead be required
254 in the post-implantation embryo for long-term silencing of germline genes. In support of this, CpGme is
255 markedly reduced at two germline gene promoters in the *Kdm5c*-KO adult hippocampus¹³.

256 Based on the above observations, we hypothesized KDM5C erases H3K4me3 to promote the initial
257 placement of CpGme at germline gene promoters in EpiLCs. To test this hypothesis, we first characterized
258 KDM5C's substrates (H3K4me2/3) at germline gene promoters in our published ChIP-seq datasets of male
259 wild-type and *Kdm5c*-KO amygdala²¹ and EpiLCs⁴¹. In congruence with the *Kdm5c*-KO hippocampus¹³,
260 we observed aberrant accumulation of H3K4me3 around the TSS of germline genes in the *Kdm5c*-KO
261 amygdala (Figure 6A). There was also a marked increase in H3K4me2 around the TSS of germline genes
262 in *Kdm5c*-KO EpiLCs (Figure 6B). To elucidate KDM5C's embryonic role, we then characterized KDM5C's
263 mRNA and protein expression during male ESC to EpiLC differentiation (Figure 6C). While *Kdm5c* mRNA
264 steadily decreased from 0 to 48 hours of differentiation (Figure 6D), KDM5C protein initially increased from
265 0 to 24 hours but then decreased to near knockout levels by 48 hours (Figure 6E). Together, these data
266 suggest KDM5C acts during the transition between ESCs and EpiLCs to remove H3K4me at germline gene
267 promoters.

268 Germline genes accumulate CpG methylation (CpGme) at CpG islands (CGIs) during the transition from
269 naïve to primed pluripotency^{19,40,65}, reaching peak methylation levels when differentiated into EpiLCs for

270 96 hours (extended EpiLCs, exEpiLCs)¹⁷. We first identified how many germline genes contained CGIs
271 using the UCSC genome browser⁶⁶ and found out of 1,288 germline-enriched genes, only 356 (27.64%)
272 had promoter CGIs (TSS ± 500 bp) (Figure 6F). CGI-containing germline genes were enriched for meiotic
273 gene ontologies, including meiotic nuclear division (GO:XXXX, p.adj) and meiosis I (GO:XXXX, p.adj) when
274 compared to CGI-free genes (Figure 6G). Although a minor portion of germline gene promoters contained
275 CGIs, CGIs strongly determined KDM5C's recruitment to germline genes (FISHER'S XXXX), with 79.15% of
276 KDM5C-bound germline genes containing CGIs (Figure 6G).

277 To assess how KDM5C loss impacts initial CpGme placement at germline gene promoters, we performed
278 whole genome bisulfite sequencing (WGBS) in male wild-type and *Kdm5c*-KO ESCs and 96 hour extended
279 EpiLCs (exEpiLCs) (Figure 6H). We first identified which germline gene promoters significantly gained
280 CpGme in wild-type cells during nESC to exEpiLCs differentiation (methylKit⁶⁷, q < 0.01, |methylation
281 difference| >= 25%, TSS ± 500 bp). In wild-type cells, the majority of germline genes gained substantial
282 CpGme at their promoter during differentiation (60.08%), regardless if their promoter contained a CGI (Figure
283 6I).

284 We then identified germline gene promoters differentially methylated in wild-type versus *Kdm5c*-KO
285 exEpiLCs (methylKit, q < 0.01, |methylation difference| > 25%, TSS ± 500 bp) and found 28 germline
286 promoters were significantly hypomethylated with *Kdm5c* loss (Figure 6J). Approximately half of germline
287 promoters hypomethylated in *Kdm5c*-KO exEpiLCs are direct targets of KDM5C in EpiLCs (13 out of 28
288 hypomethylated DMRs). Promoters that showed the most robust loss of CpGme (low q-values) harbored
289 CGIs (Figure 6J). We then evaluated promoter CpGme at germline genes ectopically transcribed in either
290 *Kdm5c*-KO EpiLCs or within the brain and found promoter CpGme was substantially reduced in about
291 half of germline DEGs (Figure 6K). Significantly hypomethylated promoters included genes consistently
292 dysregulated across multiple *Kdm5c*-KO RNA-seq datasets[], such as *Naa11* and *D1PAs1* (methylation
293 difference = -60.03%, q-value = 3.26e-153) (Figure 6L). Surprisingly, we observed only a modest reduction in
294 CpGme at *Dazl*'s promoter (methylation difference = -6.525%, q-value = 0.0159) (Figure 6M). Altogether,
295 these results demonstrate KDM5C is recruited to germline gene CGIs to promote CpGme at germline gene
296 promoters during early embryogenesis, however some loci can compensate for KDM5C loss through other
297 silencing mechanisms, even when retaining H3K4me.

298 Discussion

299 In the above study, we demonstrate KDM5C's pivotal role in the development of tissue identity. We
300 first characterized the misexpression of tissue-enriched genes within the *Kdm5c*-KO brain and identified
301 substantial dysregulation of testis, liver, muscle, and ovary-enriched genes. Testis genes significantly
302 enriched within the *Kdm5c*-KO amygdala and hippocampus are specific to germ cells and not expressed
303 within testicular somatic cells. *Kdm5c*-KO epiblast-like cells (EpiLCs) aberrantly express key drivers of

304 germline identity and meiosis, including *Dazl* and *Stra8*, while the *Kdm5c*-KO brain primarily expresses
305 genes important for late spermatogenesis. We demonstrated that while *Kdm5c* mutant sex did not influence
306 whether sperm or egg-specific genes were misexpressed, female EpiLCs are more sensitive to germline
307 gene de-repression. Germline genes can become aberrantly expressed in *Kdm5c*-KO cells via an indirect
308 mechanism, as KDM5C is only bound to a subset of germline-enriched DEGs. Finally, we found KDM5C is
309 dynamically regulated during ESC to EpiLC differentiation and promotes long-term germline gene silencing
310 through DNA methylation at CpG islands. Therefore, we propose KDM5C plays a fundamental role in
311 the development of tissue identity during early embryogenesis, including the establishment of the soma-
312 germline boundary. By systematically characterizing KDM5C's role in germline gene repression, including
313 its interaction with known silencing mechanisms, we unveiled unique repressive mechanisms governing
314 distinct classes of germline gene in somatic lineages. Furthermore, these data provide molecular footholds
315 that can then be exploited to test the ultimate contribution of ectopic germline gene expression upon
316 neurodevelopment.

317 It is important to note that while we highlighted KDM5C's regulation of germline genes, some germline-
318 enriched genes are also expressed at the 2-cell stage and in naïve ESCs for their role in pluripotency
319 and self-renewal. For example, *Dazl* is primarily known for committing PGCs to the germline fate and
320 regulating the translation of germline-specific mRNAs, but is also expressed at the 2-cell stage⁶⁸, in naïve
321 ESCs³⁷, and in the inner cell mass³⁷. Based on the de-repression of *Dazl* and *Zscan4c* in *Kdm5c*-KO
322 ESCs, KDM5C was thought to promote the 2-cell-to-ESC transition^[45]. Although expressed in naïve ESCs,
323 *Dazl* and other "self-renewal" germline genes are silenced during ESC differentiation into epiblast stem
324 cells/EpiLCs^{17,40}. We found that while *Kdm5c*-KO EpiLCs also expressed *Dazl*, they did not express 2-
325 cell specific genes. Misexpression of many germline genes in *Kdm5c*-KO EpiLCs may indicate they are
326 differentiating into primordial germ cell-like cells (PGCLCs)^{32,33,35}. Yet, *Kdm5c*-KO EpiLCs had normal
327 cellular morphology and properly expressed markers for primed pluripotency, including *Otx2* which is known
328 to repress EpiLC differentiation into PGCs/PGCLCs⁶⁹. Altogether, these data suggest *Kdm5c*-KO germline
329 gene misexpression occurs ectopically in conjunction with typical developmental programs and the 2-cell-like
330 state observed in *Kdm5c*-KO ESCs likely reflect KDM5C's primary role in germline gene repression.

331 Although eggs and sperm employ the same transcriptional programs for shared functions, e.g. PGC
332 formation, meiosis, and genome defense, some germline genes are sex specific. We found *Kdm5c* mutant
333 males and females expressed both sperm and egg-biased genes, indicating the mechanism of derepression
334 is independent of a given germline gene's sex. However, organismal sex did greatly influence the degree of
335 germline gene dysregulation, as female *Kdm5c*-KO EpiLCs had over double the number of germline-enriched
336 DEGs compared to males. The lack of X-linked gene enrichment in females suggests that this greater
337 sensitivity to germline gene misexpress is not due to XCI defects previously reported in *Kdm5c*-KO females⁴¹.
338 Sex differences in germline gene suppression may be a consequence of females having a higher dose of
339 KDM5C than males, due to its escape from XCI⁴⁸⁻⁵¹. Intriguingly, females with heterozygous loss of *Kdm5c*

340 also had over double the number of germline DEGs than hemizygous knockout males, even though their
341 level of KDM5C should be roughly equivalent to that of wild-type males. Altogether, these results suggests
342 germline gene silencing mechanisms differ between males and females, which warrants further study to
343 identify the biological implications and underlying mechanisms.

344 Emerging work indicates many histone-modifying enzymes have non-catalytic functions that influence
345 gene expression, sometimes even more potently than their catalytic roles^{70,71}. KDM5C's catalytic activity
346 may not be required for germline gene silencing, as it was recently found to be dispensable for repressing
347 *Dazl* in ESCs⁴⁵.

348 • Our results indicate KDM5C's removal of H3K4me2/3 may be necessary at a subset of CGI-containing
349 germline genes, given they fail to accumulate CpGme during EpiLC differentiation. These CpGme-
350 sensitive germline genes, such as *D1Pas1* and *Naa11*, are also de-repressed in the mature *Kdm5c*-KO
351 brain and consistently dysregulated in multiple *Kdm5c*-KO datasets¹³.

352 • H3K4me3 and CpGme typically do not colocalize
353 – <https://pubmed.ncbi.nlm.nih.gov/17334365/>
354 – <https://www.nature.com/articles/s41594-017-0013-5>
355 – <https://pubmed.ncbi.nlm.nih.gov/23664763/>
356 – <https://www.ncbi.nlm.nih.gov/pmc/articles/PMC2718496/>
357 – <https://pubmed.ncbi.nlm.nih.gov/19581485/>

358 • Contrastingly, many germline genes had only a modest reduction in CpGme, including *Dazl* even
359 though its TSS accumulated substantial H3K4me2.

360 • Multiple regulators repress *dazl*, *dazl* is not expressed in the mature *Kdm5c*-KO brain E2F6/MGA/MAX
361 - Loss of many chromatin regulators affects CpGme (Multiple, non-redundant silencing mechanisms) -
362 seems to be the crux point of germline gene silencing - Because CGIs are typically resistant to CpGme
363 (accurate?), germline CGIs may require a highly repressive histone landscape to recruit sufficient
364 DNMTs to these loci

365 • Altogether, our results indicates a given chromatin modifier's catalytic and non-catalytic regulation of
366 gene expression can change depending upon the locus and developmental stage.

367 Although the classic model for germline gene silencing is accumulation of CpGme at CGIs within their
368 promoter. We found less than 30% of germline-enriched genes have CGIs, yet the majority of CGI-free
369 germline genes still gained significant CpGme around their TSS.

370 • CGIs highly determined KDM5C recruitment to germline gene promoters.
371 • KDM5C loss also impacted CpGme at some KDM5C-unbound, CGI-free germline genes. Unclear
372 what the repressive mechanism is for these genes.

373 In somatic cells, germline genes are highly methylated at promoter CGIs, which are typically unmethylated
374 for other classes of genes.

375 • Germline gene suppression has focused on the accumulation of CpGme at CGIs

376 • DNAm and CpG islands

377 • Combine germline gene list, CGI, RFX information together.

378 – Benefit of the list is finding CGI difference and kdm5c indirect mechanisms of de-repression

379 – List of genes enables us to propose this model

380 – CGI positive meiosis/germline formation regulators turned on → these turn on CGI-negative late
381 stage regulators → These promote downstream dysregulation long term

382 • CGIs highly determine KDM5C recruitment to germline gene promoters. - KDM5C is known to be
383 enriched at CGIs (in neurons? are these methylated? or is its germline CGI function different from its
384 somatic CGI function?). - Other studies on germline gene repressors have shown they are important
385 for CGIme, unclear if they participate in non-CGI TSS CpGme

386 – Altogether demonstrates different classes of germline genes use distinct silencing mechanisms

387 It is yet unknown how KDM5C is recruited to germline gene promoters, given that KDM5C itself does
388 not contain domains for sequence-specific binding⁸. In HeLa cells and ESCs^{45,72}, KDM5C associates with
389 members of the polycomb repressive complex 1.6 (PRC1.6), which is recruited to germline gene promoters
390 through E2F6/DP1 and MGA/MAX heterodimers^{16,55}. While MAX and E2F6 motifs were enriched at KDM5C-
391 bound germline genes in EpiLCs, only about one-third of promoters contained their consensus sequence.
392 Additionally, some germline genes can become active in *Kdm5c*-KO cells independent of KDM5C binding to
393 their promoters. Germline genes unbound by KDM5C were primarily late-stage spermatogenesis genes and
394 significantly enriched for RFX transcription factors, including RFX2, a central regulator of spermiogenesis^{60,61}.
395 Another notable KDM5C-unbound DEG is *Stra8*, a meiotic transcription factor that is turned on in germ cells
396 with retionic acid signaling and DAZL expression^{73,74}. Misexpression of *Dazl* and *Rfx2* and their downstream
397 targets in *Kdm5c*-KO cells suggests that once activated, ectopic germline genes can then turn on other
398 aberrant germline programs to loosely mimic germ cell development.

399 The above work provides the mechanistic foundation for KDM5C-mediated repression of tissue and
400 germline-specific genes. However, the contribution of these ectopic, tissue-specific genes towards *Kdm5c*-
401 KO neurological impairments is still unknown. In addition to germline genes, we also identified significant
402 enrichment of muscle, liver, and even ovary-biased transcripts within the male *Kdm5c*-KO brain. Intriguingly,
403 select liver and muscle-biased DEGs do have known roles within the brain, such as the liver-enriched lipid
404 metabolism gene *Apolipoprotein C-I (Apoc1)*²⁶. *APOC1* dysregulation is implicated in Alzheimer's disease in
405 humans²⁷ and overexpression of *Apoc1* in the mouse brain can impair learning and memory⁷⁵. KDM5C may

406 therefore be crucial for neurodevelopment by fine-tuning the expression of tissue-enriched, dosage-sensitive
407 genes like *Apoc1*. Given germline genes have no known functions within the brain, their impact upon
408 neurodevelopment is currently unknown. Ectopic testicular germline transcripts have been observed in a va-
409 riety of cancers^{76,77}, including brain tumors in *Drosophila* and mammals^{78,ghafouri-fardExpressionCancerTestis2012?},
410 indicating their dysregulation may promote genome instability and cellular de-differentiation. Intriguingly,
411 some models for other chromatin-linked neurodevelopmental disorders also display impaired soma-germline
412 demarcation^{7,79-82}. Like KDM5C, the chromatin regulators underlying these conditions - DNA methyltrans-
413 ferase 3b (DNMT3B), H3K9me1/2 methyltransferases G9A/GLP, methyl-CpG -binding protein 2 (MECP2) -
414 primarily silence gene expression. Thus, KDM5C is among a growing cohort of chromatin-linked neurodevel-
415 opmental disorders with similar erosion of the germline versus soma boundary. Further research is required
416 to determine the impact of these germline genes and the extent to which this phenomenon occurs in humans.

417 Materials and Methods

418 Classifying tissue-enriched and germline-enriched genes

419 Tissue-enriched differentially expresssd genes (DEGs) were determined by their classification in a previ-
420 ously published dataset from 17 male and female mouse tissues²⁰. This study defined tissue expression as
421 greater than 1 Fragments Per Kilobase of transcript per Million mapped read (FPKM) and tissue enrichment
422 as at least 4-fold higher expression than any other tissue.

423 We curated a list of germline-enriched genes using an RNA-seq dataset from wild-type and germline-
424 depleted (Kit^{W/W^v}) male and female mouse embryos from embryonic day 12, 14, and 16³¹, as well as adult
425 male testes²⁸. Germline-enriched genes met the following criteria: 1) their expression is greater than 1
426 FPKM in wild-type germline 2) their expression in any wild-type somatic tissues²⁰ does not exceed 20%
427 of maximum expression in wild-type germline, and 3) their expression in the germ cell-depleted (Kit^{W/W^v})
428 germline, for any sex or time point, does not exceed 20% of maximum expression in wild-type germline.

429 Cell culture

430 We utilized our previously established cultures of male wild-type and *Kdm5c* knockout (-KO) embryonic
431 stem cells⁴¹. Sex was confirmed by genotyping *Uba1/Uba1y* on the X and Y chromosomes with the following
432 primers: 5'-TGGATGGTGTGCCAATG-3', 5'-CACCTGCACGTTGCCCT-3'. Deletion of *Kdm5c* was
433 confirmed through the primers 5'-ATGCCCATATTAAGAGTCCCTG-3', 5'-TCTGCCTTGATGGGACTGTT-3',
434 and 5'-GGTTCTCAACACTCACATAGTG-3'.

435 Embryonic stem cells (ESCs) and epiblast-like cells were cultured using previously established
436 methods³⁶. Briefly, ESCs were initially cultured in primed ESC (pESC) media consisting of KnockOut
437 DMEM (Gibco#10829–018), fetal bovine serum (Gibco#A5209501), KnockOut serum replacement

438 (Invitrogen#10828–028), Glutamax (Gibco#35050-061), Anti-Anti (Gibco#15240-062), MEM Non-essential
439 amino acids (Gibco#11140-050), and beta-mercaptoethanol (Sigma#M7522). They were then transitioned
440 into ground-state, “naïve” ESCs (nESCs) by culturing for four passages in N2B27 media containing
441 DMEM/F12 (Gibco#11330–032), Neurobasal media (Gibco#21103–049), Gluamax, Anti-Anti, N2 sup-
442 plement (Invitrogen#17502048), and B27 supplement without vitamin A (Invitrogen#12587-010), and
443 beta-mercaptoethanol. Both pESC and nESC media were supplemented with 3 μ M GSK3 inhibitor
444 CHIR99021 (Sigma #SML1046-5MG), 1 μ M MEK inhibitor PD0325901 (Sigma #PZ0162-5MG), and 1,000
445 units/mL leukemia inhibitory factor (LIF, Millipore#ESG1107).

446 nESCs were differentiated into epiblast-like cells (EpiLCs, 48 hours) and extendend EpiLCs (exEpiLCs,
447 96 hours) by culturing in N2B27 media containing DMEM/F12, Neurobasal media, Gluamax, Anti-Anti,
448 N2 supplement, B27 supplement (Invitrogen#17504044), beta-mercaptoethanol, fibroblast growth factor 2
449 (FGF2, R&D Biotechne 233-FB), and activin A (R&D Biotechne 338AC050CF), as previously described³⁶.

450 Immunocytochemistry (ICC)

451 ICC of DAZL in EpiLCs was performed by first growing cells on fibronectin-coated coverslips. Cells were
452 then washed thrice with phosphobuffered saline (PBS), fixed in 4% paraformaldehyde, washed thrice in PBS,
453 and blacked in PBS containing 0.3% Triton X-100, and 5% fetal bovine serum for 1 hour. They were then
454 washed thrice with PBS and incubating in primary antibody (Rabbit anti DAZL, abcam ab34139, 1:200) in
455 the blocking solution overnight at 4°C with gentle rocking. The next day, cells were rinsed thrice with PBS,
456 and incubated in secondary antibody (Alexaflouor 488 Invitrogen #710369, 1:1,000) with DAPI (1:1,000) in
457 blocking buffer for 1 hour at room temperature. Coverslips were then rinsed thrice in PBS, and mounted onto
458 slides using Prolong Gold (Invitrogen #P36930). Images were taken blinded for genotype, chosen based on
459 similar levels of DAPI signal, and quantified via ImageJ before unblinding.

460 RNA sequencing (RNA-seq)

461 After ensuring read quality via FastQC (v0.11.8), reads were then mapped to the mm10 *Mus musculus*
462 genome (Gencode) using STAR (v2.5.3a), during which we removed duplicates and kept only uniquely
463 mapped reads. Count files were generated by FeatureCounts (Subread v1.5.0), and BAM files were
464 converted to bigwigs using deeptools (v3.1.3) and visualized by the UCSC genome browser. RStudio (v3.6.0)
465 was then used to analyze counts files by DESeq2 (v1.26.0)²² to identify differentially expressed genes
466 (DEGs) with a q-value (p-adjusted via FDR/Benjamini–Hochberg correction) less than 0.1 and a log2 fold
467 change greater than 0.5. For all DESeq2 analyses, log2 fold changes were calculated with IfcShrink using
468 the ashR package⁸³. MA-plots were generated by ggpubr (v0.6.0), and Eulerr diagrams were generated by
469 eulerr (v6.1.1). Boxplots and scatterplots were generated by ggpubr (v0.6.0) and ggplot2 (v3.3.2). The Upset
470 plot was generated via the package UpSetR (v1.4.0)⁸⁴. Gene ontology (GO) analyses were performed by

471 the R package enrichPlot (v1.16.2) using the biological processes setting and compareCluster.

472 **Chromatin immunoprecipitation followed by DNA sequencing (ChIP-seq)**

473 ChIP-seq reads were aligned to mm10 using Bowtie1 (v1.1.2) allowing up to two mismatches. Only
474 uniquely mapped reads were used for analysis. Peaks were called using MACS2 software (v2.2.9.1) using
475 input BAM files for normalization, with filters for a q-value < 0.1 and a fold enrichment > 1. We removed
476 “black-listed” genomic regions that often give aberrant signals. Common peak sets were obtained in R via
477 DiffBind (v3.6.5). In the case of KDM5C ChIP-seq, *Kdm5c*-KO peaks were then subtracted from wild-type
478 samples using bedtools (v2.25.0). Peak proximity to genome annotations was determined by ChIPSeeker
479 (v1.32.1). Gene ontology (GO) analyses were performed by the R package enrichPlot (v1.16.2) using the
480 biological processes setting and compareCluster. Enriched motifs were identified using HOMER⁵⁶. Average
481 binding across the genome was visualized using deeptools (v3.1.3). Bigwigs were visualized using the
482 UCSC genome browser.

483 **Whole genome bisulfite sequencing (WGBS)**

484 Genomic DNA (gDNA) from naïve ESCs and extended EpiLCs was extracted using the Wizard Genomic
485 DNA Purification Kit (Promega A1120), following the instructions for Tissue Culture Cells. gDNA from
486 two wild-types and two *Kdm5c*-KOs of each cell type was sent to Novogene for WGBS using the Illumina
487 NovaSeq X Plus platform and sequenced for 150bp paired-end reads (PE150). - bismark - Methylkit

488 **Data availability**

489 **Published datasets**

490 All published datasets are available at the Gene Expression Omnibus (GEO) <https://www.ncbi.nlm.nih>
491 .gov/geo. Published RNA-seq datasets analyzed in this study included the male wild-type and *Kdm5c*-KO
492 adult amygdala and hippocampus²¹ (available at GEO: GSE127722) and male wild-type and *Kdm5c*-KO
493 EpiLCs⁴¹ (available at GEO: GSE96797).

494 Previously published ChIP-seq experiments included KDM5C in wild-type and *Kdm5c*-KO EpiLCs⁴¹ (avail-
495 able at GEO: GSE96797) and mouse primary neuron cultures (PNCs) from the cortex and hippocampus¹²
496 (available at GEO: GSE61036). ChIP-seq of histone 3 lysine 4 dimethylation in male wild-type and *Kdm5c*-KO
497 EpiLCs⁴¹ is also available at GEO: GSE96797. ChIP-seq of histone 3 lysine 4 trimethylation in wild-type and
498 *Kdm5c*-KO male amygdala²¹ are available at GEO: GSE127817.

499 **Data analysis**

500 Scripts used to generate the results, tables, and figures of this study are available via a GitHub repository:
501 XXX

502 **Acknowledgements**

- 503 • Jacob Mueller for providing insight in germline gene regulation.
504 • Sundeep Kalantry for providing reagents and expertise in culturing mouse embryonic stem cells and
505 epiblast-like cells
506 • Ilakkija
507 • Funding sources

508 **References**

- 509 1. Strahl, B.D., and Allis, C.D. (2000). The language of covalent histone modifications. *Nature* **403**,
510 41–45. <https://doi.org/10.1038/47412>.
- 511 2. Jenuwein, T., and Allis, C.D. (2001). Translating the Histone Code. *Science* **293**, 1074–1080.
512 <https://doi.org/10.1126/science.1063127>.
- 513 3. Lewis, E.B. (1978). A gene complex controlling segmentation in *Drosophila*. *Nature* **276**, 565–570.
514 <https://doi.org/10.1038/276565a0>.
- 515 4. Kennison, J.A., and Tamkun, J.W. (1988). Dosage-dependent modifiers of polycomb and antennapedia
516 mutations in *Drosophila*. *Proc. Natl. Acad. Sci. U.S.A.* **85**, 8136–8140. <https://doi.org/10.1073/pnas.85.21.8136>.
- 517 5. Kassis, J.A., Kennison, J.A., and Tamkun, J.W. (2017). Polycomb and Trithorax Group Genes in
518 *Drosophila*. *Genetics* **206**, 1699–1725. <https://doi.org/10.1534/genetics.115.185116>.
- 519 6. Gabriele, M., Lopez Tobon, A., D'Agostino, G., and Testa, G. (2018). The chromatin basis of
520 neurodevelopmental disorders: Rethinking dysfunction along the molecular and temporal axes. *Prog
Neuropsychopharmacol Biol Psychiatry* **84**, 306–327. <https://doi.org/10.1016/j.pnpbp.2017.12.013>.
- 521 7. Schaefer, A., Sampath, S.C., Intrator, A., Min, A., Gertler, T.S., Surmeier, D.J., Tarakhovsky, A.,
522 and Greengard, P. (2009). Control of cognition and adaptive behavior by the GLP/G9a epigenetic
suppressor complex. *Neuron* **64**, 678–691. <https://doi.org/10.1016/j.neuron.2009.11.019>.
- 523 8. Iwase, S., Lan, F., Bayliss, P., De La Torre-Ubieta, L., Huarte, M., Qi, H.H., Whetstone, J.R., Bonni, A.,
Roberts, T.M., and Shi, Y. (2007). The X-Linked Mental Retardation Gene SMCX/JARID1C Defines a
Family of Histone H3 Lysine 4 Demethylases. *Cell* **128**, 1077–1088. <https://doi.org/10.1016/j.cell.2007.02.017>.

- 524
- 525 9. Claes, S., Devriendt, K., Van Goethem, G., Roelen, L., Meireleire, J., Raeymaekers, P., Cassiman,
J.J., and Fryns, J.P. (2000). Novel syndromic form of X-linked complicated spastic paraparesis. *Am J
Med Genet* 94, 1–4.
- 526
- 527 10. Jensen, L.R., Amende, M., Gurok, U., Moser, B., Gimmel, V., Tschach, A., Janecke, A.R., Tariverdian,
G., Chelly, J., Fryns, J.P., et al. (2005). Mutations in the JARID1C gene, which is involved in
transcriptional regulation and chromatin remodeling, cause X-linked mental retardation. *Am J Hum
Genet* 76, 227–236. <https://doi.org/10.1086/427563>.
- 528
- 529 11. Carmignac, V., Nambot, S., Lehalle, D., Callier, P., Moortgat, S., Benoit, V., Ghoumid, J., Delobel,
B., Smol, T., Thuillier, C., et al. (2020). Further delineation of the female phenotype with KDM5C
disease causing variants: 19 new individuals and review of the literature. *Clin Genet* 98, 43–55.
<https://doi.org/10.1111/cge.13755>.
- 530
- 531 12. Iwase, S., Brookes, E., Agarwal, S., Badeaux, A.I., Ito, H., Vallianatos, C.N., Tomassy, G.S., Kasza, T.,
Lin, G., Thompson, A., et al. (2016). A Mouse Model of X-linked Intellectual Disability Associated with
Impaired Removal of Histone Methylation. *Cell Reports* 14, 1000–1009. [https://doi.org/10.1016/j.celr
ep.2015.12.091](https://doi.org/10.1016/j.celr
ep.2015.12.091).
- 532
- 533 13. Scandaglia, M., Lopez-Atalaya, J.P., Medrano-Fernandez, A., Lopez-Cascales, M.T., Del Blanco, B.,
Lipinski, M., Benito, E., Olivares, R., Iwase, S., Shi, Y., et al. (2017). Loss of Kdm5c Causes Spurious
Transcription and Prevents the Fine-Tuning of Activity-Regulated Enhancers in Neurons. *Cell Rep* 21,
47–59. <https://doi.org/10.1016/j.celrep.2017.09.014>.
- 534
- 535 14. Devlin, D.K., Ganley, A.R.D., and Takeuchi, N. (2023). A pan-metazoan view of germline-soma
distinction challenges our understanding of how the metazoan germline evolves. *Current Opinion in
Systems Biology* 36, 100486. <https://doi.org/10.1016/j.coisb.2023.100486>.
- 536
- 537 15. Lehmann, R. (2012). Germline Stem Cells: Origin and Destiny. *Cell Stem Cell* 10, 729–739.
<https://doi.org/10.1016/j.stem.2012.05.016>.
- 538
- 539 16. Endoh, M., Endo, T.A., Shinga, J., Hayashi, K., Farcas, A., Ma, K.W., Ito, S., Sharif, J., Endoh, T.,
Onaga, N., et al. (2017). PCGF6-PRC1 suppresses premature differentiation of mouse embryonic
stem cells by regulating germ cell-related genes. *eLife* 6. <https://doi.org/10.7554/eLife.21064>.
- 540
- 541 17. Mochizuki, K., Sharif, J., Shirane, K., Uranishi, K., Bogutz, A.B., Janssen, S.M., Suzuki, A., Okuda,
A., Koseki, H., and Lorincz, M.C. (2021). Repression of germline genes by PRC1.6 and SETDB1
in the early embryo precedes DNA methylation-mediated silencing. *Nat Commun* 12, 7020. <https://doi.org/10.1038/s41467-021-27345-x>.
- 542

- 543 18. Velasco, G., Hubé, F., Rollin, J., Neuillet, D., Philippe, C., Bouzinba-Segard, H., Galvani, A., Viegas-Péquignot, E., and Francastel, C. (2010). Dnmt3b recruitment through E2F6 transcriptional repressor mediates germ-line gene silencing in murine somatic tissues. *Proc Natl Acad Sci U S A* **107**, 9281–9286. <https://doi.org/10.1073/pnas.1000473107>.
- 544
- 545 19. Hackett, J.A., Reddington, J.P., Nestor, C.E., Dunican, D.S., Branco, M.R., Reichmann, J., Reik, W., Surani, M.A., Adams, I.R., and Meehan, R.R. (2012). Promoter DNA methylation couples genome-defence mechanisms to epigenetic reprogramming in the mouse germline. *Development* **139**, 3623–3632. <https://doi.org/10.1242/dev.081661>.
- 546
- 547 20. Li, B., Qing, T., Zhu, J., Wen, Z., Yu, Y., Fukumura, R., Zheng, Y., Gondo, Y., and Shi, L. (2017). A Comprehensive Mouse Transcriptomic BodyMap across 17 Tissues by RNA-seq. *Sci Rep* **7**, 4200. <https://doi.org/10.1038/s41598-017-04520-z>.
- 548
- 549 21. Vallianatos, C.N., Raines, B., Porter, R.S., Bonefas, K.M., Wu, M.C., Garay, P.M., Collette, K.M., Seo, Y.A., Dou, Y., Keegan, C.E., et al. (2020). Mutually suppressive roles of KMT2A and KDM5C in behaviour, neuronal structure, and histone H3K4 methylation. *Commun Biol* **3**, 278. <https://doi.org/10.1038/s42003-020-1001-6>.
- 550
- 551 22. Love, M.I., Huber, W., and Anders, S. (2014). Moderated estimation of fold change and dispersion for RNA-seq data with DESeq2. *Genome Biol* **15**, 550. <https://doi.org/10.1186/s13059-014-0550-8>.
- 552
- 553 23. Crackower, M.A., Kolas, N.K., Noguchi, J., Sarao, R., Kikuchi, K., Kaneko, H., Kobayashi, E., Kawai, Y., Kozieradzki, I., Landers, R., et al. (2003). Essential Role of Fkbp6 in Male Fertility and Homologous Chromosome Pairing in Meiosis. *Science* **300**, 1291–1295. <https://doi.org/10.1126/science.1083022>.
- 554
- 555 24. Xiol, J., Cora, E., Koglgruber, R., Chuma, S., Subramanian, S., Hosokawa, M., Reuter, M., Yang, Z., Berninger, P., Palencia, A., et al. (2012). A Role for Fkbp6 and the Chaperone Machinery in piRNA Amplification and Transposon Silencing. *Molecular Cell* **47**, 970–979. <https://doi.org/10.1016/j.molcel.2012.07.019>.
- 556
- 557 25. Cheng, S., Altmeppen, G., So, C., Welp, L.M., Penir, S., Ruhwedel, T., Menelaou, K., Harasimov, K., Stützer, A., Blayney, M., et al. (2022). Mammalian oocytes store mRNAs in a mitochondria-associated membraneless compartment. *Science* **378**, eabq4835. <https://doi.org/10.1126/science.abq4835>.
- 558
- 559 26. Rouland, A., Masson, D., Lagrost, L., Vergès, B., Gautier, T., and Bouillet, B. (2022). Role of apolipoprotein C1 in lipoprotein metabolism, atherosclerosis and diabetes: A systematic review. *Cardiovasc Diabetol* **21**, 272. <https://doi.org/10.1186/s12933-022-01703-5>.
- 560
- 561 27. Leduc, V., Jasmin-Bélanger, S., and Poirier, J. (2010). APOE and cholesterol homeostasis in Alzheimer's disease. *Trends in Molecular Medicine* **16**, 469–477. <https://doi.org/10.1016/j.molmed.2010.07.008>.
- 562

- 563 28. Mueller, J.L., Skaletsky, H., Brown, L.G., Zaghlul, S., Rock, S., Graves, T., Auger, K., Warren, W.C., Wilson, R.K., and Page, D.C. (2013). Independent specialization of the human and mouse X chromosomes for the male germ line. *Nat Genet* *45*, 1083–1087. <https://doi.org/10.1038/ng.2705>.
- 564
- 565 29. Handel, M.A., and Eppig, J.J. (1979). Sertoli Cell Differentiation in the Testes of Mice Genetically Deficient in Germ Cells. *Biology of Reproduction* *20*, 1031–1038. <https://doi.org/10.1095/biolreprod20.5.1031>.
- 566
- 567 30. Green, C.D., Ma, Q., Manske, G.L., Shami, A.N., Zheng, X., Marini, S., Moritz, L., Sultan, C., Gurczynski, S.J., Moore, B.B., et al. (2018). A Comprehensive Roadmap of Murine Spermatogenesis Defined by Single-Cell RNA-Seq. *Dev Cell* *46*, 651–667.e10. <https://doi.org/10.1016/j.devcel.2018.07.025>.
- 568
- 569 31. Soh, Y.Q., Junker, J.P., Gill, M.E., Mueller, J.L., van Oudenaarden, A., and Page, D.C. (2015). A Gene Regulatory Program for Meiotic Prophase in the Fetal Ovary. *PLoS Genet* *11*, e1005531. <https://doi.org/10.1371/journal.pgen.1005531>.
- 570
- 571 32. Magnúsdóttir, E., and Surani, M.A. (2014). How to make a primordial germ cell. *Development* *141*, 245–252. <https://doi.org/10.1242/dev.098269>.
- 572
- 573 33. Günesdogan, U., Magnúsdóttir, E., and Surani, M.A. (2014). Primordial germ cell specification: A context-dependent cellular differentiation event [corrected]. *Philos Trans R Soc Lond B Biol Sci* *369*. <https://doi.org/10.1098/rstb.2013.0543>.
- 574
- 575 34. Bardot, E.S., and Hadjantonakis, A.-K. (2020). Mouse gastrulation: Coordination of tissue patterning, specification and diversification of cell fate. *Mechanisms of Development* *163*, 103617. <https://doi.org/10.1016/j.mod.2020.103617>.
- 576
- 577 35. Hayashi, K., Ohta, H., Kurimoto, K., Aramaki, S., and Saitou, M. (2011). Reconstitution of the mouse germ cell specification pathway in culture by pluripotent stem cells. *Cell* *146*, 519–532. <https://doi.org/10.1016/j.cell.2011.06.052>.
- 578
- 579 36. Samanta, M., and Kalantry, S. (2020). Generating primed pluripotent epiblast stem cells: A methodology chapter. *Curr Top Dev Biol* *138*, 139–174. <https://doi.org/10.1016/bs.ctdb.2020.01.005>.
- 580
- 581 37. Welling, M., Chen, H., Muñoz, J., Musheev, M.U., Kester, L., Junker, J.P., Mischerikow, N., Arbab, M., Kuijk, E., Silberstein, L., et al. (2015). DAZL regulates Tet1 translation in murine embryonic stem cells. *EMBO Reports* *16*, 791–802. <https://doi.org/10.15252/embr.201540538>.
- 582
- 583 38. Macfarlan, T.S., Gifford, W.D., Driscoll, S., Lettieri, K., Rowe, H.M., Bonanomi, D., Firth, A., Singer, O., Trono, D., and Pfaff, S.L. (2012). Embryonic stem cell potency fluctuates with endogenous retrovirus activity. *Nature* *487*, 57–63. <https://doi.org/10.1038/nature11244>.
- 584

- 585 39. Suzuki, A., Hirasaki, M., Hishida, T., Wu, J., Okamura, D., Ueda, A., Nishimoto, M., Nakachi, Y.,
586 Mizuno, Y., Okazaki, Y., et al. (2016). Loss of MAX results in meiotic entry in mouse embryonic and
germline stem cells. *Nat Commun* 7, 11056. <https://doi.org/10.1038/ncomms11056>.
- 587 40. Borgel, J., Guibert, S., Li, Y., Chiba, H., Schübeler, D., Sasaki, H., Forné, T., and Weber, M. (2010).
Targets and dynamics of promoter DNA methylation during early mouse development. *Nat Genet* 42,
588 1093–1100. <https://doi.org/10.1038/ng.708>.
- 589 41. Samanta, M.K., Gayen, S., Harris, C., Maclary, E., Murata-Nakamura, Y., Malcore, R.M., Porter, R.S.,
Garay, P.M., Vallianatos, C.N., Samollow, P.B., et al. (2022). Activation of Xist by an evolutionarily
conserved function of KDM5C demethylase. *Nat Commun* 13, 2602. <https://doi.org/10.1038/s41467-022-30352-1>.
- 590 42. Koubova, J., Menke, D.B., Zhou, Q., Capel, B., Griswold, M.D., and Page, D.C. (2006). Retinoic
acid regulates sex-specific timing of meiotic initiation in mice. *Proc. Natl. Acad. Sci. U.S.A.* 103,
591 2474–2479. <https://doi.org/10.1073/pnas.0510813103>.
- 592 43. Lin, Y., Gill, M.E., Koubova, J., and Page, D.C. (2008). Germ Cell-Intrinsic and -Extrinsic Factors
Govern Meiotic Initiation in Mouse Embryos. *Science* 322, 1685–1687. <https://doi.org/10.1126/science.1166340>.
- 593 44. Endo, T., Mikedis, M.M., Nicholls, P.K., Page, D.C., and De Rooij, D.G. (2019). Retinoic Acid and Germ
594 Cell Development in the Ovary and Testis. *Biomolecules* 9, 775. <https://doi.org/10.3390/biom9120775>.
- 595 45. Gupta, N., Yakhou, L., Albert, J.R., Azogui, A., Ferry, L., Kirsh, O., Miura, F., Battault, S., Yamaguchi,
K., Laisné, M., et al. (2023). A genome-wide screen reveals new regulators of the 2-cell-like cell state.
596 *Nat Struct Mol Biol*. <https://doi.org/10.1038/s41594-023-01038-z>.
- 597 46. Pohlers, M., Truss, M., Frede, U., Scholz, A., Strehle, M., Kuban, R.-J., Hoffmann, B., Morkel, M.,
Birchmeier, C., and Hagemeier, C. (2005). A Role for E2F6 in the Restriction of Male-Germ-Cell-
598 Specific Gene Expression. *Current Biology* 15, 1051–1057. <https://doi.org/10.1016/j.cub.2005.04.060>.
- 599 47. Dahlet, T., Truss, M., Frede, U., Al Adhami, H., Bardet, A.F., Dumas, M., Vallet, J., Chicher, J.,
Hammann, P., Kottnik, S., et al. (2021). E2F6 initiates stable epigenetic silencing of germline genes
600 during embryonic development. *Nat Commun* 12, 3582. <https://doi.org/10.1038/s41467-021-23596-w>.
- 601 48. Agulnik, A.I., Mitchell, M.J., Mattei, M.G., Borsani, G., Avner, P.A., Lerner, J.L., and Bishop, C.E.
602 (1994). A novel X gene with a widely transcribed Y-linked homologue escapes X-inactivation in mouse
and human. *Hum Mol Genet* 3, 879–884. <https://doi.org/10.1093/hmg/3.6.879>.
- 603 49. Carrel, L., Hunt, P.A., and Willard, H.F. (1996). Tissue and lineage-specific variation in inactive
X chromosome expression of the murine Smcx gene. *Hum Mol Genet* 5, 1361–1366. <https://doi.org/10.1093/hmg/5.9.1361>.

- 607 50. Sheardown, S., Norris, D., Fisher, A., and Brockdorff, N. (1996). The mouse Smcx gene exhibits
developmental and tissue specific variation in degree of escape from X inactivation. *Hum Mol Genet*
608 5, 1355–1360. <https://doi.org/10.1093/hmg/5.9.1355>.
- 609 51. Xu, J., Deng, X., and Disteche, C.M. (2008). Sex-Specific Expression of the X-Linked Histone
Demethylase Gene Jarid1c in Brain. *PLoS ONE* 3, e2553. <https://doi.org/10.1371/journal.pone.00025>
610 53.
- 611 52. Wang, P.J., McCarrey, J.R., Yang, F., and Page, D.C. (2001). An abundance of X-linked genes
expressed in spermatogonia. *Nat Genet* 27, 422–426. <https://doi.org/10.1038/86927>.
- 613 53. Khil, P.P., Smirnova, N.A., Romanienko, P.J., and Camerini-Otero, R.D. (2004). The mouse X
chromosome is enriched for sex-biased genes not subject to selection by meiotic sex chromosome
614 inactivation. *Nat Genet* 36, 642–646. <https://doi.org/10.1038/ng1368>.
- 615 54. Hurlin, P.J. (1999). Mga, a dual-specificity transcription factor that interacts with Max and contains a
T-domain DNA-binding motif. *The EMBO Journal* 18, 7019–7028. <https://doi.org/10.1093/emboj/18.2>
616 4.7019.
- 617 55. Stielow, B., Finkernagel, F., Stiewe, T., Nist, A., and Suske, G. (2018). MGA, L3MBTL2 and E2F6
determine genomic binding of the non-canonical Polycomb repressive complex PRC1.6. *PLoS Genet*
618 14, e1007193. <https://doi.org/10.1371/journal.pgen.1007193>.
- 619 56. Heinz, S., Benner, C., Spann, N., Bertolino, E., Lin, Y.C., Laslo, P., Cheng, J.X., Murre, C., Singh, H.,
and Glass, C.K. (2010). Simple Combinations of Lineage-Determining Transcription Factors Prime
cis-Regulatory Elements Required for Macrophage and B Cell Identities. *Molecular Cell* 38, 576–589.
620 <https://doi.org/10.1016/j.molcel.2010.05.004>.
- 621 57. Gajiwala, K.S., Chen, H., Cornille, F., Roques, B.P., Reith, W., Mach, B., and Burley, S.K. (2000).
Structure of the winged-helix protein hRFX1 reveals a new mode of DNA binding. *Nature* 403,
622 916–921. <https://doi.org/10.1038/35002634>.
- 623 58. Swoboda, P., Adler, H.T., and Thomas, J.H. (2000). The RFX-Type Transcription Factor DAF-19
Regulates Sensory Neuron Cilium Formation in *C. elegans*. *Molecular Cell* 5, 411–421. [https://doi.org/10.1016/S1097-2765\(00\)80436-0](https://doi.org/10.1016/S1097-2765(00)80436-0).
- 625 59. Ashique, A.M., Choe, Y., Karlen, M., May, S.R., Phamluong, K., Solloway, M.J., Ericson, J., and
Peterson, A.S. (2009). The Rfx4 Transcription Factor Modulates Shh Signaling by Regional Control of
626 Ciliogenesis. *Sci. Signal.* 2. <https://doi.org/10.1126/scisignal.2000602>.
- 627 60. Kistler, W.S., Baas, D., Lemeille, S., Paschaki, M., Seguin-Estevez, Q., Barras, E., Ma, W., Duteyrat, J.-
L., Morlé, L., Durand, B., et al. (2015). RFX2 Is a Major Transcriptional Regulator of Spermiogenesis.
628 *PLoS Genet* 11, e1005368. <https://doi.org/10.1371/journal.pgen.1005368>.

- 629 61. Wu, Y., Hu, X., Li, Z., Wang, M., Li, S., Wang, X., Lin, X., Liao, S., Zhang, Z., Feng, X., et al.
630 (2016). Transcription Factor RFX2 Is a Key Regulator of Mouse Spermiogenesis. *Sci Rep* 6, 20435.
<https://doi.org/10.1038/srep20435>.
- 631 62. Liu, M., Zhu, Y., Xing, F., Liu, S., Xia, Y., Jiang, Q., and Qin, J. (2020). The polycomb group protein
632 PCGF6 mediates germline gene silencing by recruiting histone-modifying proteins to target gene
promoters. *J Biol Chem* 295, 9712–9724. <https://doi.org/10.1074/jbc.RA119.012121>.
- 633 63. Otani, J., Nankumo, T., Arita, K., Inamoto, S., Ariyoshi, M., and Shirakawa, M. (2009). Structural basis
634 for recognition of H3K4 methylation status by the DNA methyltransferase 3A ATRX–DNMT3–DNMT3L
domain. *EMBO Reports* 10, 1235–1241. <https://doi.org/10.1038/embor.2009.218>.
- 635 64. Guo, X., Wang, L., Li, J., Ding, Z., Xiao, J., Yin, X., He, S., Shi, P., Dong, L., Li, G., et al. (2015).
636 Structural insight into autoinhibition and histone H3-induced activation of DNMT3A. *Nature* 517,
640–644. <https://doi.org/10.1038/nature13899>.
- 637 65. Meissner, A., Mikkelsen, T.S., Gu, H., Wernig, M., Hanna, J., Sivachenko, A., Zhang, X., Bernstein,
638 B.E., Nusbaum, C., Jaffe, D.B., et al. (2008). Genome-scale DNA methylation maps of pluripotent and
differentiated cells. *Nature* 454, 766–770. <https://doi.org/10.1038/nature07107>.
- 639 66. Nassar, L.R., Barber, G.P., Benet-Pagès, A., Casper, J., Clawson, H., Diekhans, M., Fischer, C.,
640 Gonzalez, J.N., Hinrichs, A.S., Lee, B.T., et al. (2023). The UCSC Genome Browser database: 2023
update. *Nucleic Acids Research* 51, D1188–D1195. <https://doi.org/10.1093/nar/gkac1072>.
- 641 67. Akalin, A., Kormaksson, M., Li, S., Garrett-Bakelman, F.E., Figueiroa, M.E., Melnick, A., and Mason,
642 C.E. (2012). methylKit: A comprehensive R package for the analysis of genome-wide DNA methylation
profiles. *Genome Biol* 13, R87. <https://doi.org/10.1186/gb-2012-13-10-r87>.
- 643 68. Yang, M., Yu, H., Yu, X., Liang, S., Hu, Y., Luo, Y., Izsvák, Z., Sun, C., and Wang, J. (2022). Chemical-
induced chromatin remodeling reprograms mouse ESCs to totipotent-like stem cells. *Cell Stem Cell*
644 29, 400–418.e13. <https://doi.org/10.1016/j.stem.2022.01.010>.
- 645 69. Zhang, J., Zhang, M., Acampora, D., Vojtek, M., Yuan, D., Simeone, A., and Chambers, I. (2018).
OTX2 restricts entry to the mouse germline. *Nature* 562, 595–599. [018-0581-5](https://doi.org/10.1038/s41586-
646 018-0581-5).
- 647 70. Aubert, Y., Egolf, S., and Capell, B.C. (2019). The Unexpected Noncatalytic Roles of Histone Modifiers
648 in Development and Disease. *Trends in Genetics* 35, 645–657. <https://doi.org/10.1016/j.tig.2019.06.004>.
- 649 71. Morgan, M.A.J., and Shilatifard, A. (2020). Reevaluating the roles of histone-modifying enzymes
and their associated chromatin modifications in transcriptional regulation. *Nat Genet* 52, 1271–1281.
650 <https://doi.org/10.1038/s41588-020-00736-4>.

- 651 72. Tahiliani, M., Mei, P., Fang, R., Leonor, T., Rutenberg, M., Shimizu, F., Li, J., Rao, A., and Shi, Y.
(2007). The histone H3K4 demethylase SMCX links REST target genes to X-linked mental retardation.
652 Nature 447, 601–605. <https://doi.org/10.1038/nature05823>.
- 653 73. Endo, T., Romer, K.A., Anderson, E.L., Baltus, A.E., De Rooij, D.G., and Page, D.C. (2015). Pe-
riodic retinoic acid–STRA8 signaling intersects with periodic germ-cell competencies to regulate
654 spermatogenesis. Proc. Natl. Acad. Sci. U.S.A. 112. <https://doi.org/10.1073/pnas.1505683112>.
- 655 74. Bowles, J., Knight, D., Smith, C., Wilhelm, D., Richman, J., Mamiya, S., Yashiro, K., Chawengsak-
sophak, K., Wilson, M.J., Rossant, J., et al. (2006). Retinoid Signaling Determines Germ Cell Fate in
656 Mice. Science 312, 596–600. <https://doi.org/10.1126/science.1125691>.
- 657 75. Abildayeva, K., Berbée, J.F.P., Blokland, A., Jansen, P.J., Hoek, F.J., Meijer, O., Lütjohann, D., Gautier,
T., Pillot, T., De Vente, J., et al. (2008). Human apolipoprotein C-I expression in mice impairs learning
and memory functions. Journal of Lipid Research 49, 856–869. <https://doi.org/10.1194/jlr.M700518-JLR200>.
- 659 76. Nielsen, A.Y., and Gjerstorff, M.F. (2016). Ectopic Expression of Testis Germ Cell Proteins in Cancer
660 and Its Potential Role in Genomic Instability. Int J Mol Sci 17. <https://doi.org/10.3390/ijms17060890>.
- 661 77. Adebayo Babatunde, K., Najafi, A., Salehipour, P., Modarressi, M.H., and Mobasher, M.B. (2017).
Cancer/Testis genes in relation to sperm biology and function. Iranian Journal of Basic Medical
662 Sciences 20. <https://doi.org/10.22038/ijbms.2017.9259>.
- 663 78. Janic, A., Mendizabal, L., Llamazares, S., Rossell, D., and Gonzalez, C. (2010). Ectopic expression
of germline genes drives malignant brain tumor growth in Drosophila. Science 330, 1824–1827.
664 <https://doi.org/10.1126/science.1195481>.
- 665 79. Bonefas, K.M., and Iwase, S. (2021). Soma-to-germline transformation in chromatin-linked neurode-
666 velopmental disorders? FEBS J. <https://doi.org/10.1111/febs.16196>.
- 667 80. Velasco, G., Walton, E.L., Sterlin, D., Hédouin, S., Nitta, H., Ito, Y., Fouyssac, F., Mégarbané, A.,
Sasaki, H., Picard, C., et al. (2014). Germline genes hypomethylation and expression define a
molecular signature in peripheral blood of ICF patients: Implications for diagnosis and etiology.
668 Orphanet J Rare Dis 9, 56. <https://doi.org/10.1186/1750-1172-9-56>.
- 669 81. Walton, E.L., Francastel, C., and Velasco, G. (2014). Dnmt3b Prefers Germ Line Genes and Cen-
tromeric Regions: Lessons from the ICF Syndrome and Cancer and Implications for Diseases. Biology
670 (Basel) 3, 578–605. <https://doi.org/10.3390/biology3030578>.
- 671 82. Samaco, R.C., Mandel-Brehm, C., McGraw, C.M., Shaw, C.A., McGill, B.E., and Zoghbi, H.Y. (2012).
Crh and Oprm1 mediate anxiety-related behavior and social approach in a mouse model of MECP2
672 duplication syndrome. Nat Genet 44, 206–211. <https://doi.org/10.1038/ng.1066>.

- 673 83. Stephens, M. (2016). False discovery rates: A new deal. Biostat, kxw041. <https://doi.org/10.1093/biostatistics/kxw041>.
- 674
- 675 84. Conway, J.R., Lex, A., and Gehlenborg, N. (2017). UpSetR: An R package for the visualization of
intersecting sets and their properties. Bioinformatics 33, 2938–2940. <https://doi.org/10.1093/bioinformatics/btx364>.
- 676

677 **Figures and Tables**

- 678 • Supplementary table 1: list of all germline genes.
- 679 – Columns to include:
- 680 * KDM5C bound vs not
- 681 * DEG in EpiLC, brain, both, neither (separate columns?)



Figure 1: Tissue-enriched genes are misexpressed in the *Kdm5c*-KO brain. **A-B.** Expression of tissue-enriched genes (Li et al 2017) in the male *Kdm5c*-KO amygdala (A) and hippocampus (B). Left - MA plot of mRNA-sequencing. Right - Number of tissue-enriched differentially expressed genes (DEGs). * $p < 0.05$, ** $p < 0.01$, *** $p < 0.001$, Fisher's exact test. **C.** Left - Average bigwigs of an example aberrantly expressed testis-enriched DEG, *FK506 binding protein 6* (*Fkbp6*) in the wild-type (WT) and *Kdm5c*-KO (5CKO) amygdala (red) and hippocampus (teal). Right - Expression of *Cyct* in wild-type tissues from NCBI Gene, with testis highlighted in blue and brain tissues highlighted in red. **D.** Left - Average bigwigs of an example ovary-enriched DEG, *Zygotic arrest 1* (*Zar1*). Right - Expression of *Zar1* in wild-type tissues from NCBI Gene, with ovary highlighted in teal and brain tissues highlighted in red. **E.** Left - Average bigwigs of an example liver-enriched DEG, *Apolipoprotein C-I* (*Apoc1*). Right - Expression of *Apoc1* in wild-type tissues from NCBI Gene, with liver highlighted in orange and brain tissues highlighted in red.



Figure 2: Aberrant transcription of germline genes in the *Kdm5c*-KO in the brain. **A.** enrichPlot gene ontology (GO) of *Kdm5c*-KO amygdala and hippocampus testis-enriched DEGs **B.** Expression of testis DEGs in wild-type (WT) testis versus germ cell-depleted (W/Wv) testis (Mueller et al 2013). Expression is in Fragments Per Kilobase of transcript per Million mapped reads (FPKM). **C.** Number of testis DEGs that were classified as cell-type specific markers in a single cell RNA-seq dataset of the testis (Green et al 2018). Germline cell types are highlighted in green, somatic cell types in black. **D.** Sankey diagram of mouse genes filtered for germline enrichment based on their expression in wild-type and germline-depleted mice and in adult mouse non-gonadal tissues (Li et al 2017).

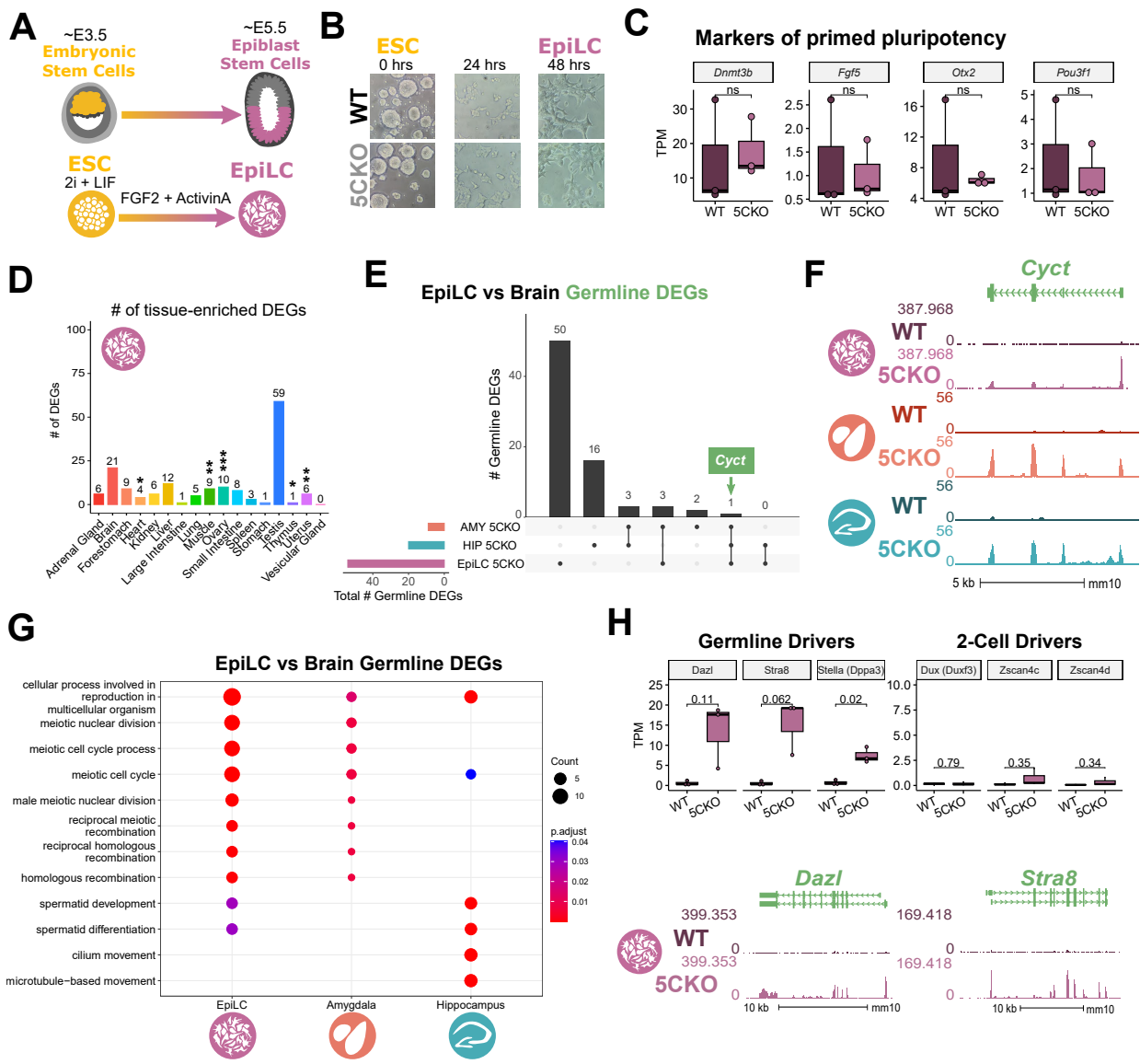


Figure 3: Kdm5c-KO epiblast-like cells express key drivers of germline identity

A. Top - Diagram of *in vivo* differentiation of embryonic stem cells (ESCs) of the inner cell mass into epiblast stem cells. Bottom - *in vitro* differentiation of ESCs into epiblast-like cells (EpiLCs).

B. Number of tissue-enriched differentially expressed genes (DEGs) in *Kdm5c*-KO EpiLCs. * $p < 0.05$, ** $p < 0.01$, *** $p < 0.001$, Fisher's exact test.

C. Average bigwigs of an example germline gene, *Cyclin T*, that is dysregulated *Kdm5c*-KO EpiLCs. Welch's t-test, expression in transcripts per million (TPM).

D. No significant difference in primed pluripotency marker expression in wild-type versus *Kdm5c*-KO EpiLCs. Welch's t-test, expression in transcripts per million (TPM).

E. Representative images of wild-type (WT) and *Kdm5c*-KO cells during ESC to EpiLC differentiation. Brightfield images taken at 20X.

F. Upset plot displaying the overlap of germline DEGs expressed in *Kdm5c*-KO EpiLCs, amygdala (AMY), and hippocampus (HIP) RNA-seq datasets.

G. enrichPlot comparing enriched biological process gene ontologies for *Kdm5c*-KO EpiLC, amygdala, and hippocampus germline DEGs.

H. Top left - Example germline identity DEGs unique to EpiLCs. Top right - Example 2-cell genes that are not dysregulated in *Kdm5c*-KO EpiLCs. p-values for Welch's t-test. Bottom - Average bigwigs of *Dazl* and *Stra8* expression in wild-type and *Kdm5c*-KO EpiLCs. Immunocytochemistry of DAZL in male wild-type (WT) and *Kdm5c*-KO (5CKO) EpiLCs. Percentage of DAZL-positive cells normalized to number of DAPI-positive cells, p-value for Welch's t-test.

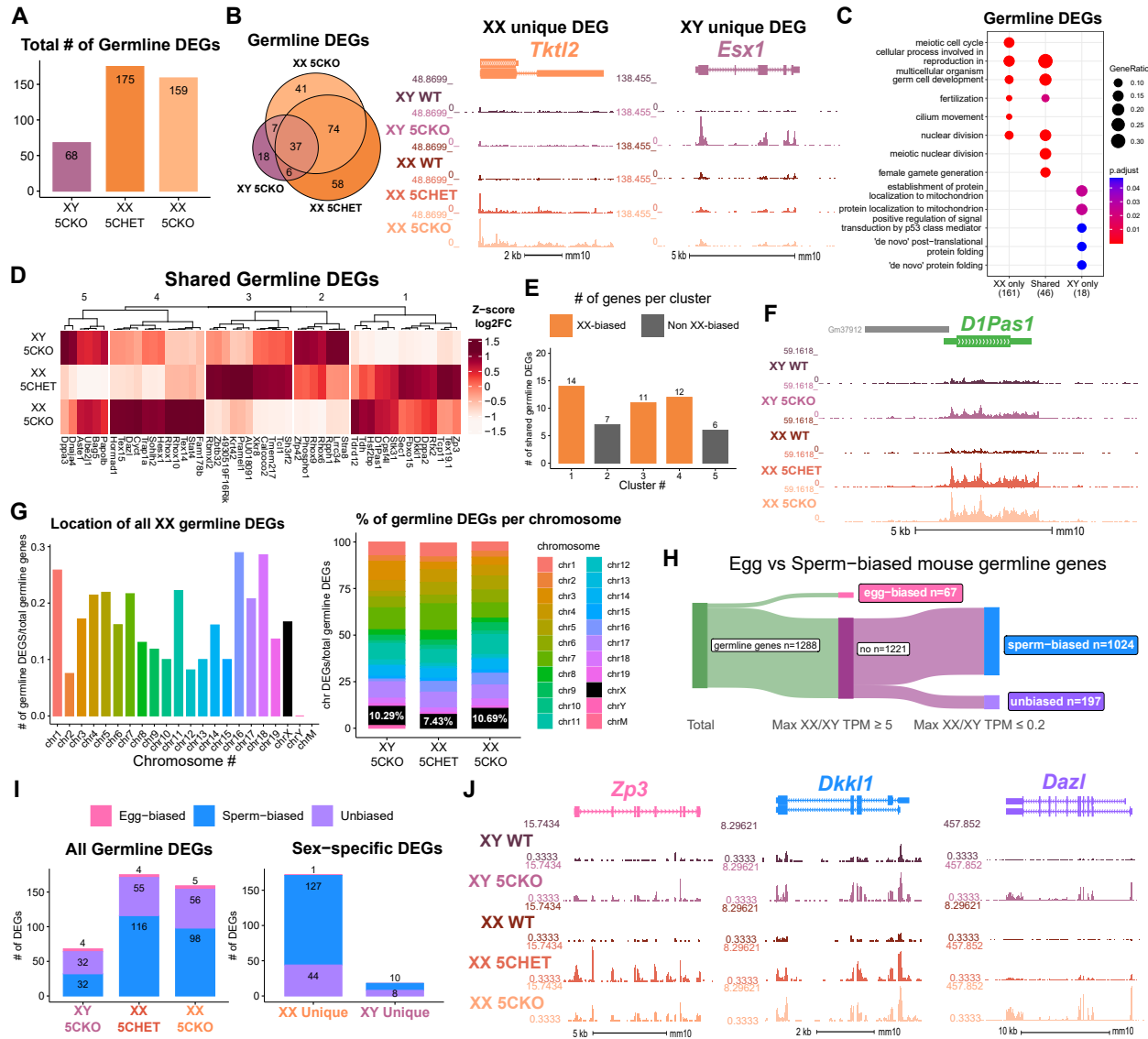


Figure 4: Chromosomal sex influences *Kdm5c*-KO germline gene misexpression. **A-B.** Expression of tissue-enriched genes (Li et al 2017) in the male *Kdm5c*-KO amygdala (A) and hippocampus (B). Left - MA plot of mRNA-seq. Right - Number of tissue-enriched differentially expressed genes (DEGs). * p<0.05, ** p<0.01, *** p<0.001, Fisher's exact test. **C.** Left - Average bigwigs of an example aberrantly expressed testis-enriched DEG, *FK506 binding protein 6* (*Fkbp6*) in the wild-type (WT) and *Kdm5c*-KO (5CKO) amygdala (red) and hippocampus (teal). Right - Expression of *Cyct* in wild-type tissues from NCBI Gene, with testis highlighted in blue and brain tissues highlighted in red. **D.** Left - Average bigwigs of an example ovary-enriched DEG, *Zygotic arrest 1* (*Zar1*). Right - Expression of *Zar1* in wild-type tissues from NCBI Gene, with ovary highlighted in teal and brain tissues highlighted in red. **E.** Left - Average bigwigs of an example liver-enriched DEG, *Apolipoprotein C-I* (*Apoc1*). Right - Expression of *Apoc1* in wild-type tissues from NCBI Gene, with liver highlighted in orange and brain tissues highlighted in red.

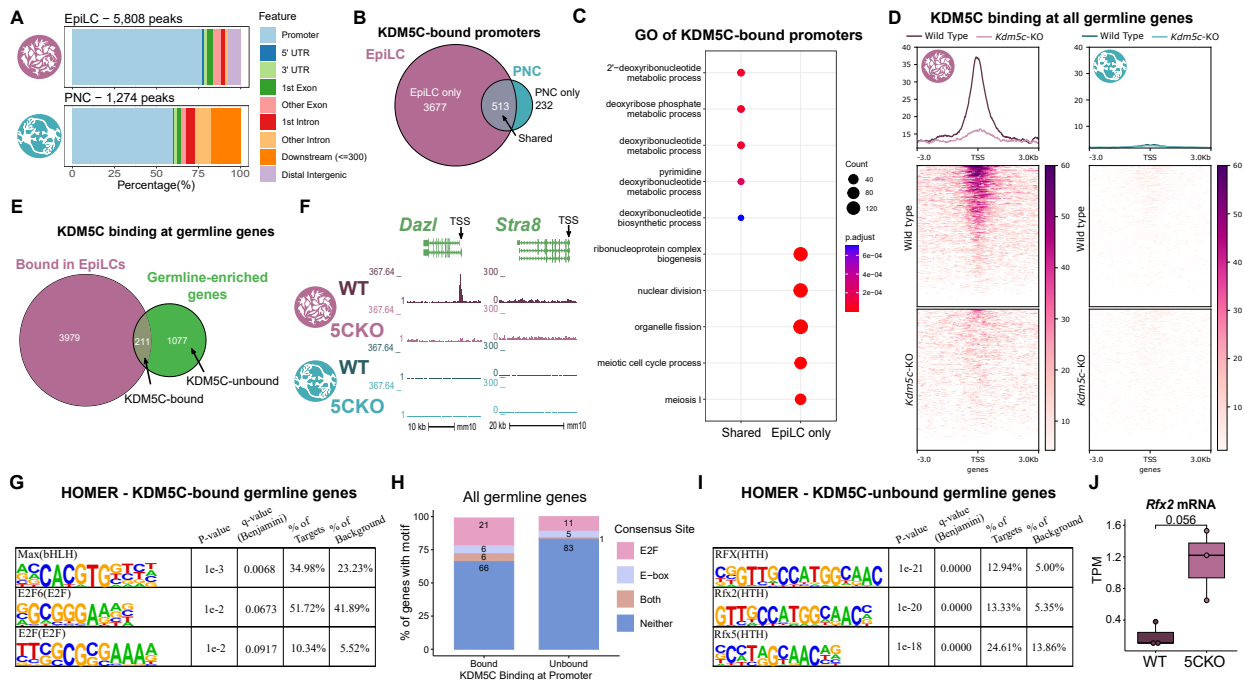


Figure 5: KDM5C binds to a subset of germline gene promoters during early embryogenesis **A.** ChIPseeker localization of KDM5C peaks at different genomic regions in EpiLCs (top) and hippocampal and cortex primary neuron cultures (PNCs, bottom). **B.** Overlap of genes with KDM5C bound to their promoters in EpiLCs (purple) and PNCs (blue). **C.** Gene ontology (GO) comparison of genes with KDM5C bound to their promoter in EpiLCs and PNCs. Genes were classified as either bound in EpiLCs only (EpiLC only), unique to PNCs (PNC only, no significant ontologies) or bound in both PNCs and EpiLCs (shared). **D.** Average KDM5C binding around the transcription start site (TSS) of all germline-enriched genes in EpiLCs (left) and PNCs (right). **E.** KDM5C binding at the promoters of RNA-seq germline DEGs. Genes were classified as either only dysregulated in EpiLCs (EpiLC only), genes dysregulated in the hippocampus or amygdala but not EpiLCs (brain only), or genes dysregulated in both EpiLCs and the brain (common). (Legend continued on next page.)

Figure 5: KDM5C binds to a subset of germline gene promoters during early embryogenesis. (Legend continued.) **F.** Example KDM5C ChIP-seq bigwigs of DEGs unique to EpiLCs. Although both are expressed in *Kdm5c*-KO EpiLCs, KDM5C is only bound to the *Dazl* promoter and not the *Stra8* promoter in EpiLCs. **G.** Example KDM5C ChIP-seq bigwigs of RNA-seq DEGs common between the brain and EpiLCs. KDM5C is bound to the *D1Pas1* promoter but not the *XXX* promoter in EpiLCs. **H.** Example KDM5C ChIP-seq bigwigs of RNA-seq DEGs unique to the brain. KDM5C is bound to the *XXX* promoter but not the *Meig1* promoter

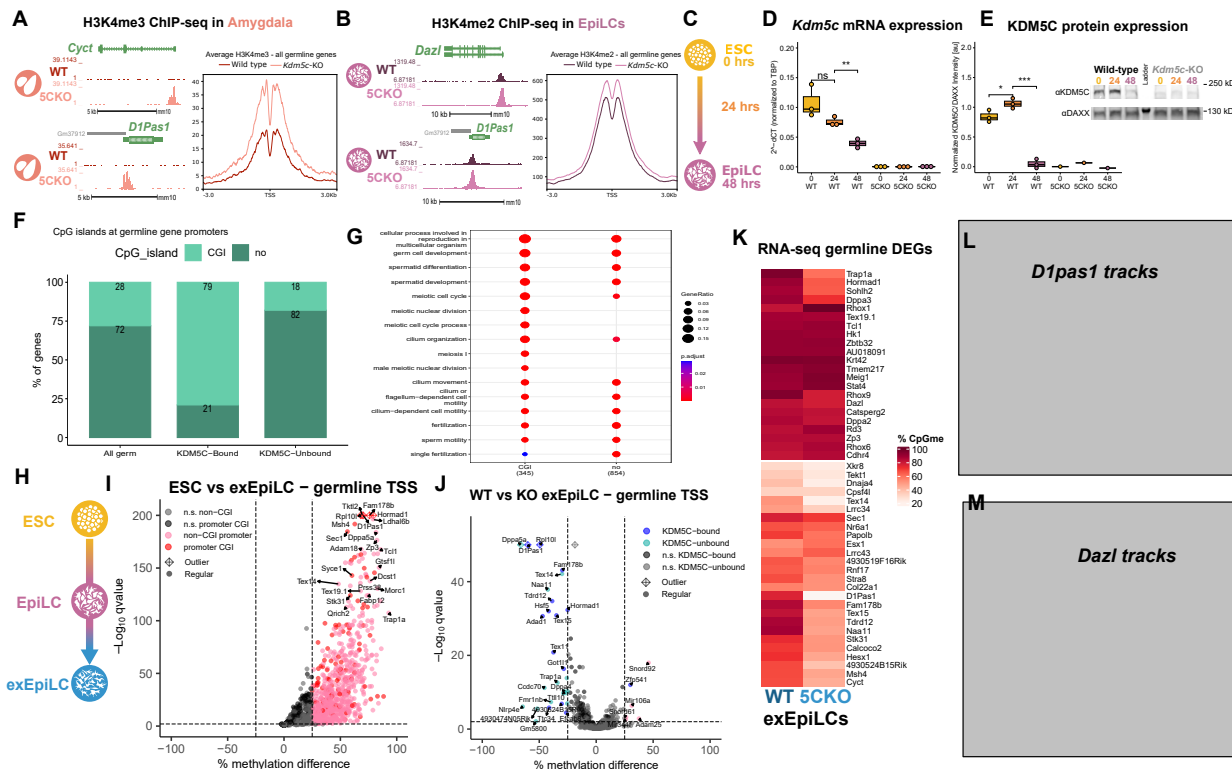


Figure 6: KDM5C's catalytic activity promotes long-term silencing of germline genes via DNA methylation. **A.** Left - Bigwigs of representative histone 3 lysine 4 trimethylation (H3K4me3) ChIP-seq peaks at two germline genes in the wild-type (WT) and *Kdm5c*-KO (5CKO) adult amygdala. Right - Average H3K4me3 at the transcription start site (TSS) of all germline-enriched genes in wild-type (dark red) and *Kdm5c*-KO (light red) amygdala. **B.** Left - Bigwigs of representative histone 3 lysine 4 dimethylation (H3K4me2) ChIP-seq peaks at representative germline genes in wild-type and *Kdm5c*-KO EpiLCs. Right - Average H3K4me2 at the TSS of all germline-enriched genes in wild-type (dark purple) and *Kdm5c*-KO (light purple) EpiLCs. **C.** Diagram of embryonic stem cell (ESC) to epiblast-like cell (EpiLC) differentiation protocol and collection time points for RNA and protein. **D.** Real time quantitative PCR (RT-qPCR) of *Kdm5c* RNA expression, calculated in comparison to TBP expression ($2^{-\Delta\Delta CT}$). * $p < 0.05$, ** $p < 0.01$, *** $p < 0.001$, Welch's t-test. **E.** KDM5C protein expression normalized to DAXX. Quantified intensity using ImageJ (artificial units - au). Right - representative lanes of Western blot for KDM5C and DAXX. * $p < 0.05$, ** $p < 0.01$, *** $p < 0.001$, Welch's t-test **F.** XXX **G.** XXX